

# Lattice Approach to Excited TBA Boundary Flows: Tricritical Ising Model

Giovanni Feverati<sup>1</sup>, Paul A. Pearce<sup>2</sup>

*Department of Mathematics and Statistics  
University of Melbourne, Parkville, Victoria 3010, Australia*

Francesco Ravanini<sup>3</sup>

*INFN Sezione di Bologna, Dipartimento di Fisica  
Via Irnerio 46, 40126 Bologna, Italy*

## Abstract

We show how a lattice approach can be used to derive Thermodynamic Bethe Ansatz (TBA) equations describing all excitations for boundary flows. The method is illustrated for a prototypical flow of the tricritical Ising model by considering the continuum scaling limit of the  $A_4$  lattice model with integrable boundaries. Fixing the bulk weights to their critical values, the integrable boundary weights admit two boundary fields  $\xi$  and  $\eta$  which play the role of the perturbing boundary fields  $\varphi_{1,3}$  and  $\varphi_{1,2}$  inducing the renormalization group flow between boundary fixed points. The excitations are completely classified in terms of  $(\mathbf{m}, \mathbf{n})$  systems and quantum numbers but the string content changes by certain mechanisms along the flow. For our prototypical example, we identify these mechanisms and the induced map between the relevant finitized Virasoro characters. We also solve the boundary TBA equations numerically to determine the flows for the leading excitations.

## 1 Introduction

A problem of much current interest in Quantum Field Theory (QFT) is the renormalization group (RG) flow between different boundary fixed points of a Conformal Field Theory (CFT) that remains conformal in the bulk. Many boundary flows have been studied including [1, 2] Lee-Yang, minimal models and  $c = 1$  CFTs. In addition, approximate numerical scaling energies can be explored by use of the Truncated Conformal Space Approach (TCSA) [3].

In this letter, for boundary flows, we show how one can derive exact TBA equations [4] for all excitations from a lattice approach [5, 6, 7, 8]. This has not been possible in a field theory approach. We illustrate our approach in the context of a prototypical boundary flow of the Tricritical Ising Model (TIM) [9, 10] with central charge  $c = 7/10$ . This is an interesting but relatively simple CFT with many applications in statistical mechanics. Following Cardy [11], the conformal boundary conditions  $B_{(r,s)}$  of the TIM are in one-to-one

---

<sup>1</sup>feverati@ms.unimelb.edu.au

<sup>2</sup>P.Pearce@ms.unimelb.edu.au

<sup>3</sup>ravanini@bologna.infn.it

correspondence with the six primary fields  $\varphi_{(r,s)} \equiv \varphi_{(4-r,5-s)}$  labelled by the Kac labels  $(r,s)$  with  $r = 1, 2, 3$  and  $s = 1, 2, 3, 4$ . The Kac table of conformal weights  $\Delta_{r,s}$  is shown in Figure 1. Of the many possible flows on a cylinder between boundary conditions  $B_{(r,s)|(r',s')}$  (that is  $B_{(r,s)}$  on the left and  $B_{(r',s')}$  on the right) we only consider here flows involving a non-trivial boundary  $B_{(r,s)}$  on the left with a fixed trivial boundary  $B_{(1,1)}$  on the right. For these conformal boundary conditions on the cylinder we use the special notation

$$\mathcal{B}_{(r,s)} = B_{(r,s)|(1,1)}.$$

In Figure 1 the possible integrable flows [10] between these conformal boundary conditions are shown schematically.

$s$				
2	$\frac{1}{10}$	$\frac{3}{80}$	$\frac{3}{5}$	
1	0	$\frac{7}{16}$	$\frac{3}{2}$	
	1	2	3	$r$

Figure 1: Kac table of conformal weights  $\Delta_{r,s} = ((5r - 4s)^2 - 1)/80$  of the tricritical Ising model. We restrict to the lower half of the table with  $s = 1, 2$  using the usual identification  $(r,s) \equiv (4 - r, 5 - s)$ . The integrable flows between the six conformal boundary conditions  $\mathcal{B}_{(r,s)}$  are shown schematically. The  $\varphi_{(1,3)}$  and  $\varphi_{(1,2)}$  flows are indicated by solid and dotted arrows respectively. We omit non-Cardy type boundary conditions.

In this letter we will focus on the prototypical flow obtained by perturbing the  $\mathcal{B}_{(1,2)}$  boundary TIM by the relevant boundary operator  $\varphi_{(1,3)}$

$$UV = \mathcal{B}_{(1,2)} \mapsto \mathcal{B}_{(2,1)} = IR, \quad \chi_{1,2}(q) \mapsto \chi_{2,1}(q) \quad (1.1)$$

This flow induces a map between Virasoro characters  $\chi_{r,s}(q)$  of the theory where  $q$  is the modular parameter. The physical direction of the flow from the ultraviolet (UV) to the infrared (IR) is given by the relevant perturbations and is consistent with the  $g$ -theorem [12] which asserts that the boundary entropy is reduced under the flow  $g_{IR} < g_{UV}$ . The boundary entropies are

$$g_{(r,s)} = \left(\frac{2}{5}\right)^{1/4} \frac{\sin \frac{\pi r}{4} \sin \frac{\pi s}{5}}{\sqrt{\sin \frac{\pi}{4} \sin \frac{\pi}{5}}}, \quad g_{(1,1)} : g_{(2,1)} : g_{(1,2)} : g_{(2,2)} = 1 : \sqrt{2} : g : \sqrt{2}g \quad (1.2)$$

with  $g = (1 + \sqrt{5})/2$  the golden mean.

A more complete account of the full set of six integrable flows of the TIM, including the second flow emanating from the  $\mathcal{B}_{(1,2)}$  boundary condition, will be given in a subsequent paper [13]. The approach outlined here, however, is quite general and should apply, for example, to all integrable boundary flows of minimal models [14].

## 2 Scaling of Critical $A_4$ Model with Boundary Fields

It is well known that the TIM is obtained as the continuum scaling limit of the generalized hard square model of Baxter [15] on the Regime III/IV critical line. This integrable lattice model is the  $A_4$  RSOS lattice model of Andrews-Baxter-Forrester [16]. Specifically, in the presence of integrable boundaries, the scaling energies of the TIM are obtained [6] from the scaling limit of the eigenvalues of the commuting double-row transfer matrices  $\mathbf{D}(u)$  [17] of the  $A_4$  lattice model with  $N$  faces in a row. It has been shown by Behrend and Pearce [18] that at criticality there exist integrable boundary conditions associated with each conformal boundary condition  $(r, s)$  carrying 0, 1 or 2 arbitrary boundary fields  $\xi, \eta$ . In the present case the boundaries  $(1, 1)$  and  $(3, 1)$  admit no fields,  $(2, 1)$  and  $(1, 2)$  admit a single field  $\xi$  and  $(2, 2)$  admits two boundary fields  $\xi$  and  $\eta$ . These boundary fields induce the  $\varphi_{(1,3)}$  and  $\varphi_{(1,2)}$  RG flows respectively so we identify the thermal and magnetic boundary fields accordingly

$$\xi \sim \varphi_{(1,3)}, \quad \eta \sim \varphi_{(1,2)}. \quad (2.1)$$

To consider boundary flows we must fix the bulk at its critical point and vary the boundary fields  $\xi, \eta$ . But paradoxically, it has been shown [6] that the fields  $\xi, \eta$  are irrelevant in the sense that they do not change the scaling energies if  $\xi$  and  $\eta$  are real and restricted to appropriate intervals. Explicitly, the cylinder partition functions obtained [6, 18] from  $(r, s)$  integrable boundaries with  $\xi, \eta$  real are independent of  $\xi, \eta$  and given by single Virasoro characters

$$\mathcal{B}_{(r,s)} = B_{(r,s)|(1,1)} : \quad Z_{(r,s)|(1,1)}(q) = \chi_{r,s}(q). \quad (2.2)$$

The reason for this is that in the lattice model the fields  $\xi$  and  $\eta$  control the location of zeros on the real axis in the complex plane of the spectral parameter  $u$  whereas only the zeros in the scaling regime, a distance  $i \log N$  out from the real axis, contribute in the scaling limit  $N \rightarrow \infty$ . The solution is to scale the imaginary part of  $\xi, \eta$  as  $\log N$ . This is allowed because  $\xi, \eta$  are arbitrary complex fields.

For our prototypical flow (1.1), following [6, 18], we consider a cylindrical lattice with the  $(1, 1)$  boundary on the right (with no boundary field) and the  $(2, 1)$  boundary on the left with boundary field  $\xi_L$ . Explicitly, we now scale  $\xi_L$  as

$$\text{Re}(\xi_L) = \frac{\lambda}{2} = \frac{\pi}{5}, \quad \text{Im}(\xi_L) = \frac{-\xi + \log N}{5} \quad (2.3)$$

where  $\xi$  is real. In terms of boundary weights, the  $(1, 2)$  conformal boundary is reproduced in the limit  $\text{Im}(\xi_L) \rightarrow \pm\infty$  whereas the  $(2, 1)$  conformal boundary is reproduced in the limit  $\text{Im}(\xi_L) \rightarrow 0$ .

The scaling behaviour of the  $A_4$  lattice model at the boundary fixed points is described by the TBA equations of O'Brien, Pearce and Warnaar [6] (OPW). In this letter, we generalize their analysis to include the scaling boundary field (2.3). This parameter appears in the TBA equations only through the boundary contribution  $g(u)$  in (6.3) of OPW. For the flow (1.1), the scaling limit of this function in the first analyticity strip  $-\frac{\lambda}{2} \leq \text{Re}(u) \leq \frac{3\lambda}{2}$  now becomes

$$\hat{g}_1(x, \xi) = \coth \frac{x + \xi}{2} \quad (2.4)$$

with  $\xi \rightarrow -\infty$  and  $\xi \rightarrow +\infty$  corresponding to  $\mathcal{B}_{(1,2)}$  and  $\mathcal{B}_{(2,1)}$  respectively.

### 3 Classification and Flow of Excited States $\mathcal{B}_{(1,2)} \mapsto \mathcal{B}_{(2,1)}$

As in OPW, the scaling energies are classified by the patterns of zeros of the eigenvalues of the double row transfer matrix  $\mathbf{D}(u)$ . In the complex  $u$  plane, they are organized in two analyticity strips  $-\frac{\lambda}{2} \leq \text{Re}(u) \leq \frac{3\lambda}{2}$  and  $2\lambda \leq \text{Re}(u) \leq 4\lambda$ . For  $N$  sufficiently large, there can be only simple zeros in the middle of each strip (1-strings) or pairs of zeros located on the two borders of each strip, having the same imaginary part (2-strings). Because of crossing symmetry, all the zeros appear in complex conjugate pairs so the upper and lower half planes are related by reflection in the real axis and this remains true for general values of  $\text{Im}(\xi_L)$ .

The patterns of zeros are classified [6] by string content and ordering. Let  $m_{1,2} \geq 0$  be the number of 1-strings in the upper half plane in strips 1 and 2 and similarly  $n_{1,2} \geq 0$  the number of 2-strings. Then for the boundary fixed points  $\mathcal{B}_{(1,2)}$  and  $\mathcal{B}_{(2,1)}$ , the string contents are classified by the  $(\mathbf{m}, \mathbf{n})$  systems

$$UV = \mathcal{B}_{(1,2)} \text{ (} m_1 \text{ odd, } m_2 \text{ even)} : \quad n_1 = \frac{N+m_2+\sigma}{2} - m_1, \quad n_2 = \frac{m_1 - \sigma}{2} - m_2 \quad (3.1)$$

$$IR = \mathcal{B}_{(2,1)} \text{ (} m_1 \text{ odd, } m_2 \text{ odd)} : \quad n_1 = \frac{N+m_2}{2} - m_1, \quad n_2 = \frac{m_1 + 1}{2} - m_2 \quad (3.2)$$

where  $N$  is odd. In the UV there are two distinct  $(\mathbf{m}, \mathbf{n})$  systems labelled by  $\sigma = \pm 1$ . In the scaling limit  $N \rightarrow \infty$ , we have  $n_1 \sim N/2$  with  $m_1, m_2, n_2 = O(1)$ . For given string content, the relative ordering of 1- and 2- strings is given by the quantum numbers  $I_k^{(i)}$  where, for the 1-string  $y_k^{(i)}$ ,  $I_k^{(i)}$  is the number of two-strings whose location  $z_l^{(i)}$  is larger (further from the real axis) than  $y_k^{(i)}$ . Labelling the strings so that  $y_{k+1}^{(i)} > y_k^{(i)}$ , the quantum numbers must satisfy

$$n_i \geq I_1^{(i)} \geq I_2^{(i)} \geq \dots \geq I_{m_i}^{(i)} \geq 0. \quad (3.3)$$

In  $\mathcal{B}_{(1,2)}$  with  $\sigma = 1$  there is a frozen 1-string, that is, the 1-string furthest from the real axis in strip 1 is restricted to have no two-strings above it so that  $I_{m_1}^{(1)} = 0$ . With these quantum numbers, the states are uniquely labelled as

$$UV = \mathcal{B}_{(1,2)} : \quad I = (I_1^{(1)} I_2^{(1)} \dots I_{m_1}^{(1)} | I_1^{(2)} I_2^{(2)} \dots I_{m_2}^{(2)})_\sigma \quad (3.4)$$

$$IR = \mathcal{B}_{(2,1)} : \quad I = (I_1^{(1)} I_2^{(1)} \dots I_{m_1}^{(1)} | I_1^{(2)} I_2^{(2)} \dots I_{m_2}^{(2)}) \quad (3.5)$$

In the scaling limit,  $n_1$  is infinite so in this limit the corresponding strip 1 quantum numbers are unbounded.

Given the pattern of zeros, that is, the string content and quantum numbers at the boundary fixed points, the conformal dimensions or scaling energies of these states are uniquely determined [6] by

$$UV = \mathcal{B}_{(1,2)} : \quad E = \Delta_{(1,2)} + n^{UV} = \frac{1}{10} + \frac{1}{4} \mathbf{m} C \mathbf{m} - \frac{m_1 - m_2}{2} \sigma + \sum_{i=1,2} \sum_{k=1, \dots, m_i} I_k^{(i)} \quad (3.6)$$

$$IR = \mathcal{B}_{(2,1)} : \quad E = \Delta_{(2,1)} + n^{IR} = \frac{7}{16} - \frac{1}{2} + \frac{1}{4} \mathbf{m} C \mathbf{m} + \sum_{i=1,2} \sum_{k=1, \dots, m_i} I_k^{(i)} \quad (3.7)$$

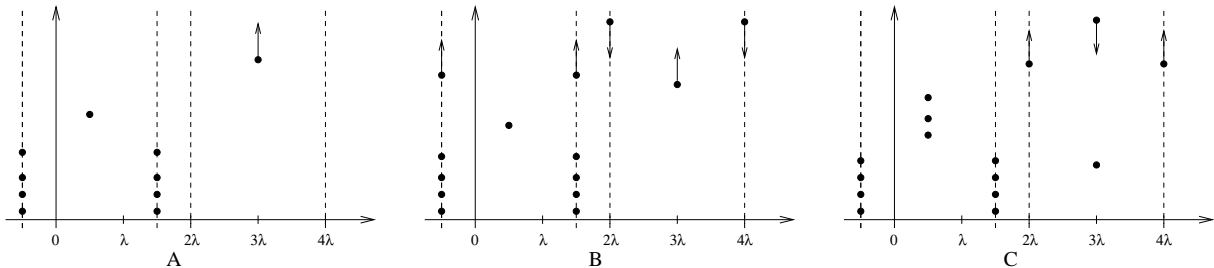


Figure 2: The three mechanisms A, B, C respectively that change string content during the flow  $\mathcal{B}_{(2,1)} \mapsto \mathcal{B}_{(1,2)}$ . Note that this is the reverse of the physical flow. These mechanisms are illustrated for the states: A,  $(0|0) \mapsto (0)_+$ ; B,  $(1|0) \mapsto (0)_-$ ; C,  $(000|1) \mapsto (000|00)_-$ .

where  $\mathbf{m} = (m_1, m_2)$  and the Cartan matrix is

$$C = \begin{pmatrix} 2 & -1 \\ -1 & 2 \end{pmatrix} \quad (3.8)$$

From [6], we know that the above counting of states reproduces exactly the expected UV and IR characters at the boundary fixed points but there must be some mechanisms to change these classifications during the flow.

### 3.1 Three mechanisms for changing string content

For convenience, in this section only, we consider the flow  $IR = \mathcal{B}_{(2,1)} \mapsto \mathcal{B}_{(1,2)} = UV$  which is the reverse of the physical flow (1.1). By simple counting arguments, the eigenvalues of the double row transfer matrix have  $2N + 4$  zeros in the periodicity strip for  $\mathcal{B}_{(2,1)}$  but only  $2N + 2$  zeros for  $\mathcal{B}_{(1,2)}$ . Thus precisely two zeros, one in the upper half plane and one in the lower half plane, must “flow off to infinity” during the flow. Indeed, from empirical observations based on direct numerical diagonalization of small double row transfer matrices we find just three mechanisms for changing the string content during the flow. These all involve the farthest zeros (1 or 2 strings) from the real axis in the upper half plane and are well supported by numerical analysis of the TBA equations in Section 5.

The mechanisms for the flow  $IR = \mathcal{B}_{(2,1)} \mapsto \mathcal{B}_{(1,2)} = UV$ , as shown in Figure 2, are:

- A. The top 1-string in strip 2 flows to  $+\infty$ , decoupling from the system while  $m_1$ ,  $n_1$  and  $n_2$  remain unchanged. This mechanism applies in the IR when  $I_{m_1}^{(1)} = I_{m_2}^{(2)} = 0$  and produces frozen states in the UV with  $\sigma = 1$  and  $I_{m_1}^{(1)} = 0$ .
- B. The top 2-string in strip 1 and the top 1-string in strip 2 flow to  $+\infty$  and a 2-string comes in from  $+\infty$  in strip 2 becoming the top 2-string. Consequently, each  $I_j^{(1)}$  decreases by 1 and each  $I_k^{(2)}$  increases by 1. This mechanism applies in the IR when  $I_{m_1}^{(1)} > 0$  and  $I_{m_2}^{(2)} = 0$  and produces states in the UV with  $\sigma = -1$  and either  $m_2 = 0$  or  $I_{m_2}^{(2)} > 0$ .
- C. The top 2-string in strip 2 flows to  $+\infty$  and a 1-string in strip 2 comes in from  $+\infty$ . Consequently, each  $I_k^{(2)}$  decreases by 1. This mechanism applies in the IR when  $I_{m_2}^{(2)} > 0$  and produces states in the UV with  $\sigma = -1$  and  $I_{m_2}^{(2)} = 0$ .

Observe that these mappings are in fact one-to-one, that the 1-strings in strip 1 are never involved in these mechanisms and that the change in parity of  $m_2$  is consistent with (3.1) and (3.2)

$$A, B : m_2^{UV} = m_2^{IR} - 1, \quad C : m_2^{UV} = m_2^{IR} + 1 \quad (3.9)$$

The explicit mapping of the first 18 states is shown in Table 1. The consistency and completeness of these three mechanisms is demonstrated by the explicit mapping between the finitized characters associated with the UV and IR fixed points. The situation here is very similar to the massless thermal  $\varphi_{1,3}$  flow [8] from the TIM to the critical Ising model and is best described in terms of finitized Virasoro characters [19].

$n$	Mapping of states and mechanism		$n$	Mapping of states and mechanism	
0	$(0)_+ \mapsto (0 0)$	A	5	$(4)_- \mapsto (5 0)$	B
1	$(0)_- \mapsto (1 0)$	B	5	$(110)_+ \mapsto (110 0)$	A
2	$(1)_- \mapsto (2 0)$	B	5	$(200)_+ \mapsto (200 0)$	A
3	$(2)_- \mapsto (3 0)$	B	6	$(110 00)_- \mapsto (110 1)$	C
3	$(000)_+ \mapsto (000 0)$	A	6	$(200 00)_- \mapsto (200 1)$	C
4	$(000 00)_- \mapsto (000 1)$	C	6	$(5)_- \mapsto (6 0)$	B
4	$(3)_- \mapsto (4 0)$	B	6	$(000)_- \mapsto (111 0)$	B
4	$(100)_+ \mapsto (100 0)$	A	6	$(210)_+ \mapsto (210 0)$	A
5	$(100 00)_- \mapsto (100 1)$	C	6	$(300)_+ \mapsto (300 0)$	A

Table 1: Explicit mapping of states in the order of increasing energy for the first 18 energy levels, where  $n = n^{UV} = n^{IR}$  is the excitation level as in (3.6) and (3.7). For some higher levels  $n^{UV} \neq n^{IR}$ .

### 3.2 RG mapping between finitized characters

Finitized characters are the generating functions for the scaling energies of the  $A_4$  model for finite  $M \times N$  lattices:

$$\chi_{r,s}^{(N)}(q) = q^{-c/24} \sum_E q^E = q^{-c/24} \text{Tr} \left( \frac{\mathbf{D}^{(N)}(u)}{D_0^{(N)}(u)} \right)^{M/2} \quad (3.10)$$

where the modular parameter is  $q = \exp(-\pi \sin(5u)M/N)$  and  $D_0^{(N)}(u)$  is the largest eigenvalue of the double-row transfer matrix  $\mathbf{D}^{(N)}(u)$  with  $(r, s)$  boundary conditions. The finitized characters involve Gaussian polynomials which satisfy a recursion used repeatedly below

$$\begin{bmatrix} m+n \\ m \end{bmatrix} = \sum_{I_1=0}^n \sum_{I_2=0}^{I_1} \cdots \sum_{I_m=0}^{I_{m-1}} q^{I_1+\dots+I_m}, \quad \begin{bmatrix} n \\ m \end{bmatrix} = \begin{bmatrix} n-1 \\ m-1 \end{bmatrix} + q^m \begin{bmatrix} n-1 \\ m \end{bmatrix} \quad (3.11)$$

Let us return to the map induced by the physical flow  $UV = \mathcal{B}_{(1,2)} \mapsto \mathcal{B}_{(2,1)} = IR$ . We can write the UV finitized character as

$$\begin{aligned}
\chi_{(1,2)}^{(N)}(q) &= q^{-\frac{c}{24} + \frac{1}{10}} \sum_{\sigma, m_1, m_2^{UV}} q^{\frac{1}{4} \mathbf{m}^{UV} C \mathbf{m}^{UV}} q^{-\frac{\sigma}{2} (m_1 - m_2^{UV})} \begin{bmatrix} m_1 + n_1^{UV} - \delta_{\sigma,1} \\ m_1 - \delta_{\sigma,1} \end{bmatrix} \begin{bmatrix} m_2^{UV} + n_2^{UV} \\ m_2^{UV} \end{bmatrix} \\
&= q^{-\frac{c}{24} + \frac{1}{10}} \sum_{m_1, m_2^{UV}} q^{\frac{1}{4} \mathbf{m}^{UV} C \mathbf{m}^{UV}} \left\{ q^{-\frac{1}{2} (m_1 - m_2^{UV})} \begin{bmatrix} N + m_2^{UV} - 1 \\ m_1 - 1 \end{bmatrix} \begin{bmatrix} \frac{m_1 - 1}{2} \\ m_2^{UV} \end{bmatrix} \right. \\
&\quad \left. + q^{\frac{1}{2} (m_1 - m_2^{UV})} \begin{bmatrix} N + m_2^{UV} - 1 \\ m_1 \end{bmatrix} \left( q^{m_2^{UV}} \begin{bmatrix} \frac{m_1 - 1}{2} \\ m_2^{UV} \end{bmatrix} + \begin{bmatrix} \frac{m_1 - 1}{2} \\ m_2^{UV} - 1 \end{bmatrix} \right) \right\} \quad (3.12)
\end{aligned}$$

where the three terms correspond to the three mechanisms A, B, C respectively. This is confirmed by simple counting in the limit  $q \rightarrow 1$  when the Gaussian polynomials reduce to binomials. Here  $m_1 = m_1^{UV} = m_1^{IR}$  does not change under the flow. Assuming (3.6), (3.7) and mechanisms A, B, C hold for all  $N$  we can uniquely map,  $q^{E^{UV}} \mapsto q^{E^{IR}}$ , energy level by energy level. In effect, this means we replace  $m_2^{UV}$  with  $m_2^{IR}$  using (3.9) and the energies at the base of each Gaussian tower change according to

$$A: \quad q^{\frac{1}{4} \mathbf{m}^{UV} C \mathbf{m}^{UV} - \frac{1}{2} (m_1 - m_2^{UV})} \mapsto q^{\frac{1}{4} \mathbf{m}^{IR} C \mathbf{m}^{IR} - \frac{1}{2}} \quad (3.13)$$

$$B: \quad q^{\frac{1}{4} \mathbf{m}^{UV} C \mathbf{m}^{UV} + \frac{1}{2} (m_1 + m_2^{UV})} \mapsto q^{\frac{1}{4} \mathbf{m}^{IR} C \mathbf{m}^{IR} - \frac{1}{2}} q^{m_1} \quad (3.14)$$

$$C: \quad q^{\frac{1}{4} \mathbf{m}^{UV} C \mathbf{m}^{UV} + \frac{1}{2} (m_1 - m_2^{UV})} \mapsto q^{\frac{1}{4} \mathbf{m}^{IR} C \mathbf{m}^{IR} - \frac{1}{2}} q^{m_2^{IR}} \quad (3.15)$$

Putting all this together we obtain the desired mapping between finitized characters

$$\begin{aligned}
\chi_{(1,2)}^{(N)}(q) &\mapsto q^{-\frac{c}{24} + \frac{7}{16} - \frac{1}{2}} \sum_{m_1, m_2^{IR}} q^{\frac{1}{4} \mathbf{m}^{IR} C \mathbf{m}^{IR}} \left\{ \begin{bmatrix} N + m_2^{IR} - 2 \\ m_1 - 1 \end{bmatrix} \begin{bmatrix} \frac{m_1 - 1}{2} \\ m_2^{IR} - 1 \end{bmatrix} \right. \\
&\quad \left. + q^{m_1} \begin{bmatrix} N + m_2^{IR} - 2 \\ m_1 \end{bmatrix} \begin{bmatrix} \frac{m_1 - 1}{2} \\ m_2^{IR} - 1 \end{bmatrix} + q^{m_2^{IR}} \begin{bmatrix} N + m_2^{IR} \\ m_1 \end{bmatrix} \begin{bmatrix} \frac{m_1 - 1}{2} \\ m_2^{IR} \end{bmatrix} \right\} \quad (3.16) \\
&= q^{-\frac{c}{24} + \frac{7}{16} - \frac{1}{2}} \sum_{m_1, m_2^{IR}} q^{\frac{1}{4} \mathbf{m}^{IR} C \mathbf{m}^{IR}} \begin{bmatrix} N + m_2^{IR} \\ m_1 \end{bmatrix} \left( \begin{bmatrix} \frac{m_1 - 1}{2} \\ m_2^{IR} - 1 \end{bmatrix} + q^{m_2^{IR}} \begin{bmatrix} \frac{m_1 - 1}{2} \\ m_2^{IR} \end{bmatrix} \right) \\
&= q^{-\frac{c}{24} + \frac{7}{16} - \frac{1}{2}} \sum_{m_1, m_2^{IR}} q^{\frac{1}{4} \mathbf{m}^{IR} C \mathbf{m}^{IR}} \begin{bmatrix} N + m_2^{IR} \\ m_1 \end{bmatrix} \begin{bmatrix} \frac{m_1 + 1}{2} \\ m_2^{IR} \end{bmatrix} = \chi_{(2,1)}^{(N)}(q)
\end{aligned}$$

## 4 Boundary TBA Equations $\mathcal{B}_{(1,2)} \mapsto \mathcal{B}_{(2,1)}$

The derivation of TBA equations is a straightforward extension of OPW to include the  $\xi$ -dependent boundary term (2.4). The TBA equations are

$$\epsilon_1(x) = -\log \hat{g}_1(x, \xi) - \sum_{j=1}^{m_1} \log \tanh\left(\frac{y_j^{(1)} - x}{2}\right) - K * \log(1 - e^{-\epsilon_2(x)}) \quad (4.1)$$

$$\epsilon_2(x) = 4e^{-x} - \sum_{k=1}^{m_2} \log \tanh\left(\frac{y_k^{(2)} - x}{2}\right) - K * \log(1 - e^{-\epsilon_1(x)}) \quad (4.2)$$

where  $*$  denotes convolution, the kernel is  $K(x) = 1/(2\pi \cosh x)$  and the auxiliary variables  $y_k^{(i)}$  denote the scaled location of the 1-strings in strip  $i$ . Similarly, the scaling energies  $E(\xi)$  are

$$E(\xi) - \frac{c}{24} = \frac{1}{\pi} \lim_{R \rightarrow 0} RE(R) = \frac{1}{\pi} \left[ \sum_{j=1}^{m_1} 2e^{-y_j^{(1)}} - \int_{-\infty}^{\infty} \frac{dx}{\pi} e^{-x} \log(1 - e^{-\epsilon_2(x)}) \right] \quad (4.3)$$

where the limit  $R \rightarrow 0$  means that all these computations are performed at the critical temperature of the TIM. For the lowest level  $E(\xi)$  interpolates between the conformal weights  $\Delta = 1/10$  and  $7/16$  at the boundary fixed points.

As in OPW the auxiliary variables  $y_k^{(i)}$  are determined by a set of auxiliary equations determining the locations of the 1-strings

$$\epsilon_2(y_j^{(1)} - i\frac{\pi}{2}) = n_j^{(1)} i\pi, \quad \text{1-strings in strip 1} \quad (4.4)$$

$$\epsilon_1(y_k^{(2)} - i\frac{\pi}{2}) = n_k^{(2)} i\pi, \quad \text{1-strings in strip 2} \quad (4.5)$$

where  $n_k^{(i)}$  are given in the IR by the *quantization conditions*

$$n_j^{(1)} = 2(m_1 - j + I_j^{(1)}) + 1 - m_2, \quad j = 1, 2, \dots, m_1 \quad (4.6)$$

$$n_k^{(2)} = 2(m_2 - k + I_k^{(2)}) + 1 - m_1, \quad k = 1, 2, \dots, m_2 \quad (4.7)$$

The integers  $n_k^{(i)}$  can change during the flow due to winding of phases. The appropriate form in the UV is given in OPW. Observe that the boundary field  $\xi$  appears explicitly only in the function  $\hat{g}_1$ .

The 2-strings do not appear in the TBA equations. However, they are involved in mechanisms B and C. To follow the movement of 2-strings along the flow we note that their locations  $z_k^{(i)}$  satisfy the same equations (4.4), (4.5) with the substitution  $y_k^{(i)} \rightarrow z_k^{(i)}$  and the appropriate choice of the quantum numbers. We note that in general, and in particular for the TIM, it remains an open problem in this approach to obtain the  $g$ -function flow [1, 20] that interpolates between the boundary entropies (1.2) at the fixed points.



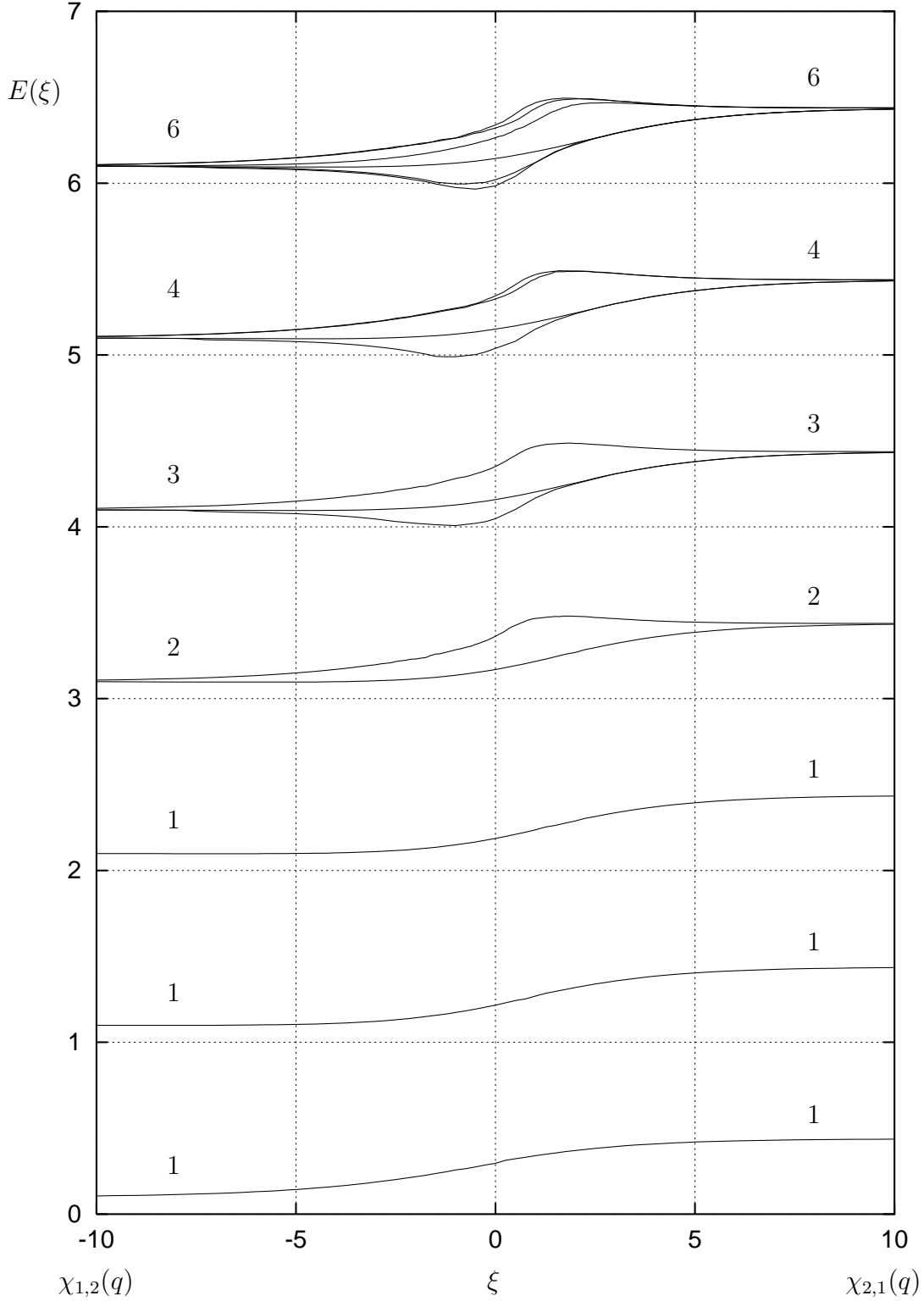


Figure 3: The flow of scaling energies  $E(\xi)$  between the  $\mathcal{B}_{(1,2)}$  and  $\mathcal{B}_{(2,1)}$  boundary fixed points as obtained by the numerical solution of the TBA equations. Only scaling energies with  $\Delta < 7$  are shown as in Table 1. The indicated degeneracies in the UV (left) and IR (right) are consistent with the degeneracies of the Virasoro characters  $\chi_{1,2}(q) = \chi_{1/10}(q)$  and  $\chi_{2,1}(q) = \chi_{7/16}(q)$  respectively.

## 5 Numerical Analysis of the RG Flow $\mathcal{B}_{(1,2)} \mapsto \mathcal{B}_{(2,1)}$

The TBA equations of the previous section can be solved numerically by an iterative procedure but there are some subtleties. The process starts with an initial guess, for the pseudoenergies  $\epsilon_i(x)$  and 1-string locations, close to the UV or IR fixed points. The flow is followed by progressively incrementing or decrementing the boundary field  $\xi$ . At each value of  $\xi$ , the TBA equations are used to update the pseudoenergies  $\epsilon_i(x)$  and then these are used in the auxiliary equations to update the locations of the 1-strings, and so on, until a stable solution is reached. In our preliminary numerical study we have considered all the states with  $\Delta < 7$  as shown in Figure 3. The corresponding mappings of UV and IR quantum numbers and the mechanisms responsible are listed in Table 1. These flows, and in particular the behaviour of the 1- and 2-strings, confirm the mechanisms A, B, C.

The most important new feature of the numerics is the existence, due to the term (2.4), of a pole at  $x = -\xi$  which marches through the center of the analyticity strip 1 as  $\xi$  is varied. This leads to some inherent numerical instabilities as the pole successively encounters the 1-string locations in strip 1. A second numerical problem is related to the determination of the location of the 1-strings in strip 2. This problem was previously encountered in [8] and arises because  $y_k^{(2)}$  cannot be obtained by direct iteration of the auxiliary equation. It is partially solved here using two different schemes

1. Inverting certain phases containing  $y_j^{(1)} - y_k^{(2)}$ .
2. Inverting the boundary term that contains  $y_k^{(2)} - \xi$ .

The first method, used with success in [6], can be sensitive to errors in the location of  $y_j^{(1)}$ . The second method ties  $y_k^{(2)}$  to  $\xi$  so it is generally less sensitive to errors in  $y_j^{(1)}$ . Usually both schemes converge to the same results but in some regions we find one scheme converges where the other fails.

## Acknowledgements

This work is supported by the ARC and INFN. Part of this work was done during visits of FR to Melbourne and GF and PAP to Bologna and IPAM, UCLA. We thank these institutes for their support. We thank P. Dorey, G. Mussardo, V. Rittenberg and R. Tateo for reading the manuscript.

## References

- [1] A. LeClair, G. Mussardo, H. Saleur and S. Skorik, Nucl. Phys. **B453** (1995) 581.
- [2] P. Dorey, A. Pocklington, R. Tateo and G.M.T. Watts, Nucl. Phys. **B525** (1998) 641; P. Dorey, M. Pillin, A. Pocklington, I. Runkel, R. Tateo, G.M.T. Watts, hep-th/0010278 (2000); K. Graham, I. Runkel and G.M.T. Watts, Nucl. Phys. **B608** (2001) 527.
- [3] V.P. Yurov and Al.B. Zamolodchikov, Int. J. Mod. Phys. **A5** (1990) 3221.

- [4] C.N. Yang and C.P. Yang, J. Math. Phys. **10** (1969) 1115; A.I.B. Zamolodchikov, Nucl. Phys. **B342** (1990) 695; Nucl. Phys. **B358** (1991) 497; Nucl. Phys. **B358** (1991) 524; Nucl. Phys. **B366** (1991) 122.
- [5] P.A. Pearce and A. Klümper, Phys. Rev. Lett. **66** (1991) 974; A. Klümper and P.A. Pearce, J. Stat. Phys. **64** (1991) 13; A. Klümper and P.A. Pearce, Physica **A183** (1992) 304.
- [6] D.L. O'Brien, P.A. Pearce and S.O. Warnaar, Nucl. Phys. **B501**, 773 (1997).
- [7] P.A. Pearce and B. Nienhuis, Nucl. Phys. **B519** (1998) 579.
- [8] P.A. Pearce, L. Chim and C. Ahn, Nucl. Phys. **B601** (2001) 539; *Excited TBA Equations II: Massless Flow from Tricritical to Critical Ising Model*, in preparation (2002).
- [9] L. Chim, J. Math. Phys. **A11** (1996) 4491; K. Graham, I. Runkel and G.M.T. Watts, hep-th/0010082, Talk given at *Nonperturbative Quantum Effects 2000*.
- [10] A. Recknagel, D. Roggenkamp, V. Schomerus, Nucl. Phys. **B588** (2000), 552; I. Affleck, J. Phys. **A33** (2000) 6473.
- [11] J.L. Cardy, Nucl. Phys. **B324** (1989) 481.
- [12] I. Affleck and A. Ludwig, Phys. Rev. Lett. **67** (1991) 161.
- [13] G. Feverati, P.A. Pearce and F. Ravanini, *Excited TBA Boundary Flows in the Tricritical Ising Model*, in preparation (2002).
- [14] A.A. Belavin, A.M. Polyakov and A.B. Zamolodchikov, Nucl. Phys. **B241** (1984) 333.
- [15] R.J. Baxter, J. Phys. **A13** (1980) L61; R.J. Baxter, "Exactly Solved Models in Statistical Mechanics", Academic Press, London, 1982; R.J. Baxter and P.A. Pearce, J. Phys. **A15** (1982) 897; J. Phys. **A16** (1983) 2239.
- [16] G.E. Andrews, R.J. Baxter and P.J. Forrester, J. Stat. Phys. **35** (1984) 193.
- [17] R.E. Behrend, P.A. Pearce and D.L. O'Brien, J. Stat. Phys. **84**, 1 (1996).
- [18] R.E. Behrend and P.A. Pearce, J. Phys. A **29** (1996), 7827; Int. J. Mod. Phys. **B11** (1997) 2833; J. Stat. Phys. **102** (2001) 577.
- [19] E. Melzer, Int. J. Mod. Phys. **A9** (1994) 1115; A. Berkovich, Nucl. Phys. **B431** (1994) 315.
- [20] P. Dorey, I. Runkel, R. Tateo, G.M.T. Watts, Nucl. Phys. **B578** (2000) 85.